Multi-Physics Capabilities in SU2

Beckett Y. Zhou[1]

... and many others in the SU2 Community

[1]Chair for Scientific Computing, TU Kaiserslautern, Germany

SU2

The Open-Source CFD Code

August 9, 2019

Aeroacoutics

Contributors:

- Beckett Y. Zhou, Tim Albring, Nicolas Gauger (TU Kaiserslautern)
- Carlos R. da Silva (Embraer S. A.)
- Thomas D. Economon (Bosch)
- Juan Alonso (Stanford University)
- Hua-Dong Yao, Shia-Hui Peng, Lars Davidson (Chalmers)
- Leonard V. Lopes (NASA Langley)
- Omur Icke, Andy Moy, Oktay Baysal (Old Dominion University)
- Boris Diskin (NIA)

Point of Contact:

Beckett Y. Zhou: yuxiang.zhou@scicomp.uni-kl.de

Aeroacoustic Simulation and Optimization in SU2

Turbulent Flow Simulation

- URANS
- DDES

Acoustic Propagation

- 2D: frequency-domain permeable-surface Ffowcs Williams-Hawkings (FWH) of Lockard, 2000
- 3D: time-domain solid- and permeable-surface FWH (Formulation F1A of Farassat)

Special for Broadband Noise

- RANS coupled with stochastic noise generation (SNG)

Adjoint-based Optimization

- Coupled URANS-FWH/RANS-SNG discrete adjoint based on algorithmic differentiation (AD)

Aeroacoustic Simulation and Optimization in SU2 – The Past, Present, and Future

Initial Work

- 2D URANS+FWH in frequency domain
- Noise minimization on various 2D configurations

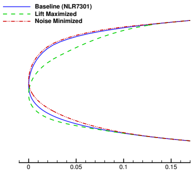

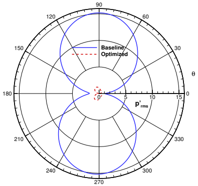

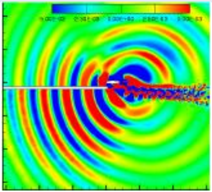

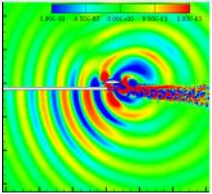

AVIATION 2016 (AIAA 2016-3369)

SCI-TECH 2017 (AIAA 2017-0130)

Aeroacoustic Simulation and Optimization in SU2 – The Past, Present, and Future

Initial Work

- 2D URANS+FWH in frequency domain
- Noise minimization on various 2D configurations

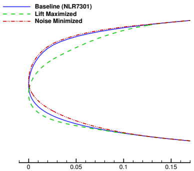

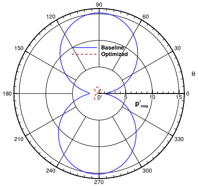

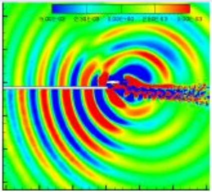

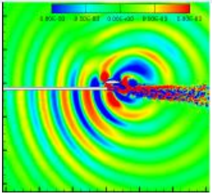

Ph.D. Thesis

- 3D fixed-source FWH, coupled with URANS and DDES
- Noise minimization with 3D URANS+FWH, final analysis using DDES+FWH
- Preliminary validation against experiment using DDES+FWH

Current

- Extension to moving-source FWH in 3D (Formulation F1A of Farassat)
- (U)RANS with stochastic noise generation (RANS-SNG)

Coupled CFD-FWH Noise Prediction and Optimization Framework

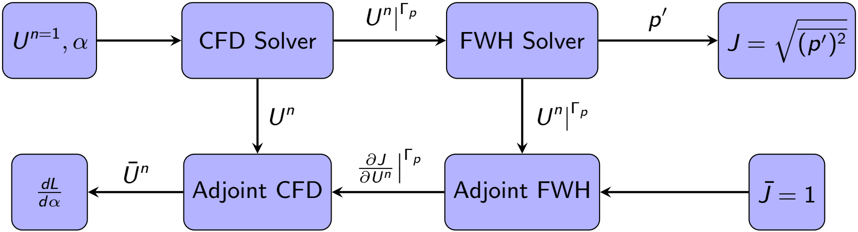

- CFD Solver: $U^n = G^n(U^n, U^{n-1}, U^{n-2})$
- FWH Solver: $p'_{obs}(\vec{x}, t) = p'_T + p'_L = Fn(\,U\big|^{\Gamma_p}, \vec{x}, t)$
- Adjoint CFD: $\bar{U}^n = \bar{G}^n(\bar{U}^n, \bar{U}^{n-1}, \bar{U}^{n-2}) + (\,\frac{\partial J}{\partial U^n}\Big|^{\Gamma_p})^T$
- $U^n\big|^{\Gamma_p}$: Flow variables at time step n on the FWH surface Γ_p
- $\frac{\partial J}{\partial U^n}\Big|^{\Gamma_p}$: sensitivity of the noise objective with respect to flow variables evaluated on the FWH surface Γ_p

Aeroacoustic Simulation and Optimization in SU2

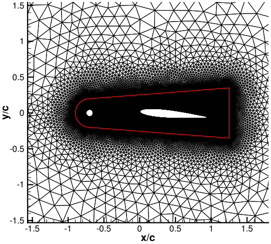

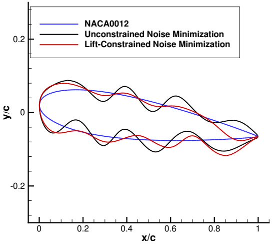

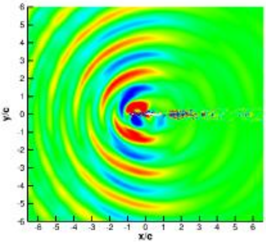

Baseline Rod-Airfoil

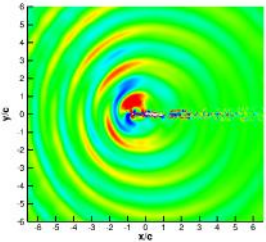

Unconstrained Noise Min.

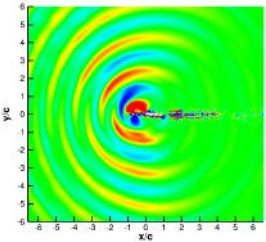

Lift-Constrained Noise Min.

Aeroacoustic Simulation and Optimization in SU2

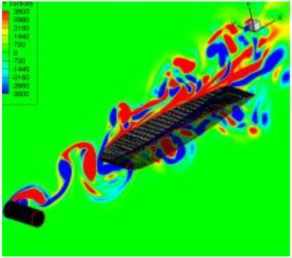

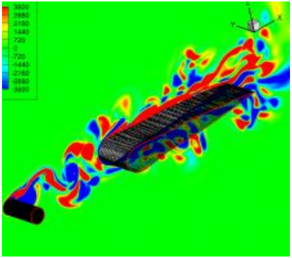

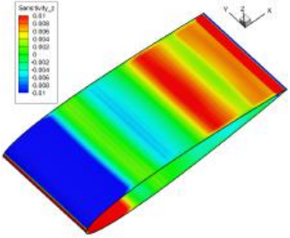

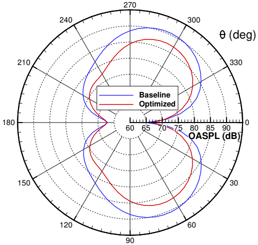

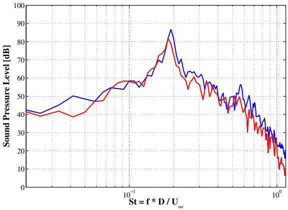

Extension to 3D Moving-Source FWH

- Fixed-source FWH extended to full F1A formulation of Farassat
- Test case: rotating and translating sphere ($M_\infty = 0.5$, RPM=812 about $\hat{x}$)
- URANS-FWH result validated against static CFD pressure and NASA-ANOPP2

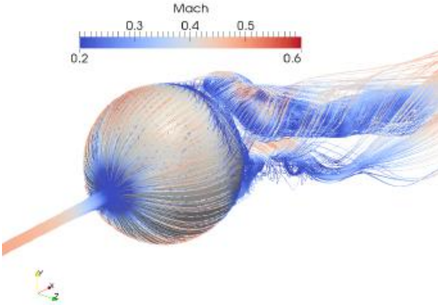

$R = 10D$

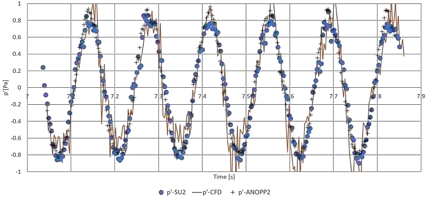

$R = 150D$

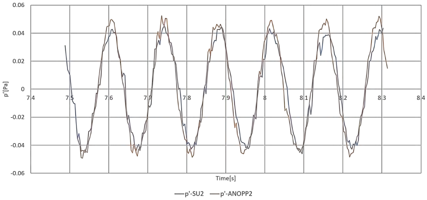

*On-Going Work: **Omur Icke**, Andy Moy, Beckett Y. Zhou, Oktay Baysal, Leonard V. Lopes and Boris Diskin

RANS-SNG Broadband Noise Assessment Framework

Basic Idea

Use stochastic noise generation (SNG) to reconstruct the turbulent velocity field based on turbulence kinetic energy (TKE) and dissipation rates (ϵ or ω) estimated by a preceding RANS computation.

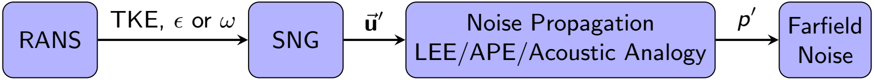

- Pioneering work in RANS-SNG by Bechara et al. and Bailly et al. in the 1990s
- Method improved by the works of Billson et al., Casalino and Barbarino, and di Francescantonio et al. in recent years.
- Similar idea to the RANS-RPM approach of Ewert et al. (circa. 2000)

What RANS-SNG Method IS and ISN'T

- NOT designed to predict broadband noise to an *absolute* level
- Fast assessment of broadband noise source characteristics and trends for design optimization
- A method to circumvent the regularization issue plaguing adjoint solutions for scale-resolving simulations

Trailing-Edge Noise Minimization (SciTech 2019)

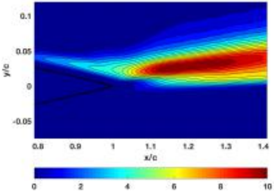

Baseline NACA0012

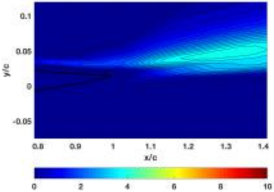

Optimized w/o $\frac{C_L}{C_D}$ Constr.

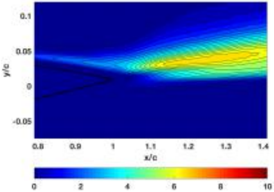

Optimized w/ $\frac{C_L}{C_D}$ Constr.

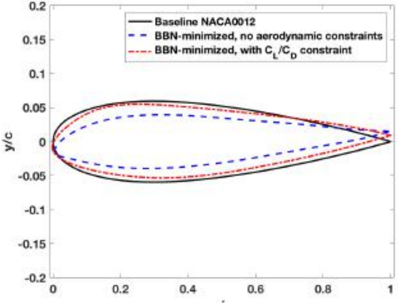

- BBN source minimization performed with and without aerodynamic constraint
- Shape optimization effectively reduces trailing-edge broadband noise source
- In progress: verification of results with scale-resolving simulations
- Details in: AIAA-2019-0002

Flap Side Edge Broadband Noise Minimization

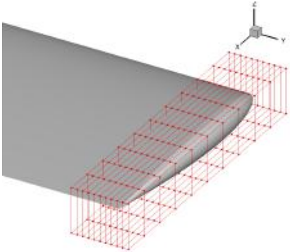

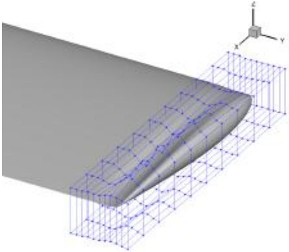

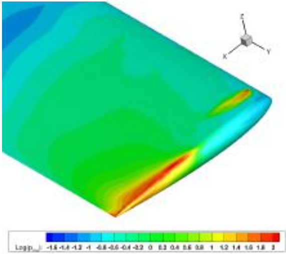

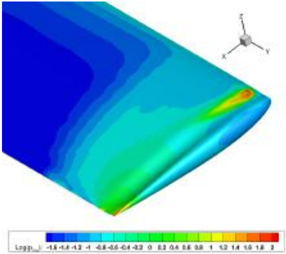

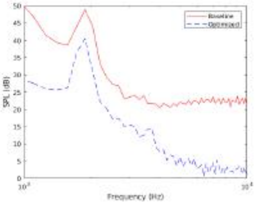

Aeroacoustic Simulation and Optimization in SU2

Reference Publications

- **B. Y. Zhou**, T. Albring, N. R. Gauger, C. R. da Silva, T. D. Economon, and J. J. Alonso, "*An Efficient Airframe Noise Reduction Framework via Adjoint-based Shape Optimization*", AIAA Journal (Submitted)
- **B. Y. Zhou**, N. R. Gauger, H. Yao, S. Peng, and L. Davidson, "*Adjoint-based Broadband Noise Minimization using Stochastic Noise Generation*", In 25th AIAA/CEAS Aeroacoustics Conference, No. 2019-2697, Delft, 2019.
- **B. Y. Zhou**, T. Albring, N. R. Gauger, C. R. da Silva, T. D. Economon, and J. J. Alonso, "*Reduction of Airframe Noise Components Using a Discrete Adjoint Approach*", In 18th AIAA/ISSMO Multidisciplinary Analysis and Optimization Conference, No. 2017-3658, Denver, CO, 2017.
- **B. Y. Zhou**, T. Albring, N. R. Gauger, C. R. da Silva, T. D. Economon, and J. J. Alonso, "*A Discrete Adjoint Approach for Jet-Flap Interaction Noise Reduction*", In 58th AIAA/ASCE/AHS/ASC Structures, Structural Dynamics, and Materials Conference, No. 2017-0130, Grapevine, TX, 2017
- **B. Y. Zhou**, T. Albring, N. R. Gauger, T. D. Economon, F. Palacios, and J. J. Alonso, "*A Discrete Adjoint Framework for Unsteady Aerodynamic and Aeroacoustic Optimization*", In 16th AIAA/ISSMO Multidisciplinary Analysis and Optimization Conference, No. 2015-3355, Dallas, TX, 2015.

Future Work

- Aeroacoustic optimization of rotor and propeller blades
- Propagation of SNG noise source using high-order SU2-DG solver
- Machine learning for SNG using LES data

Fluid-Structure Interaction

Contributors:

- Rubén Sánchez, Tim Albring, Nicolas Gauger (TU Kaiserslautern)
- Pedro Gomez, Joel Ho Munn Onn, Rafael Palacios (Imperial College London)
- Thomas D. Economon (Bosch)
- Juan Alonso (Stanford University)

Point of Contact:

Rubén Sánchez: ruben.sanchez@scicomp.uni-kl.de

Coupled FSI Solver

- ➔ Fully Implicit, coupled solver
- ➔ ALE Formulation
- ➔ Geometrical Non-Linearities
- ➔ Complex material model
- ➔ Consistent interpolation on domain-filling discretizations
- ➔ Elastic solver for mesh movement
- ➔ Fully differentiated using AD

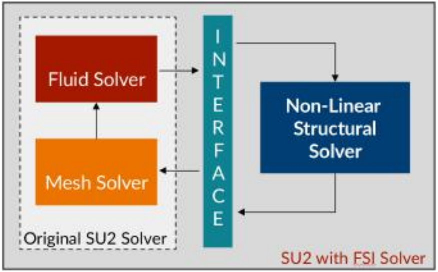

First Paper:

R. Sanchez, R. Palacios, T.D. Economon, H.L. Kline, J.J. Alonso and F. Palacios, "*Towards a Fluid-Structure Interaction Solver for Problems with Large Deformations Within the Open-Source SU2 Suite*", AIAA paper 2016-0205, presented at Scitech 2016

Coupled FSI Solver

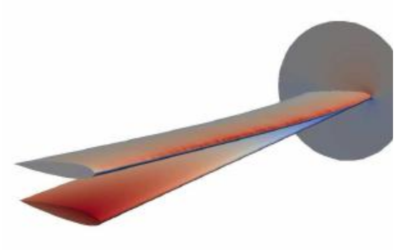

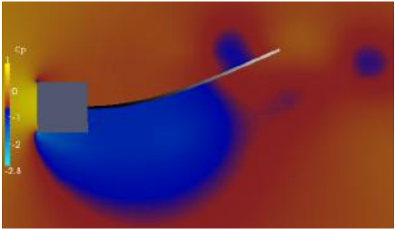

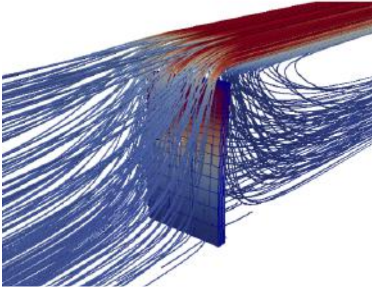

Coupled FSI Adjoint Solver based on Algorithmic Differentiation

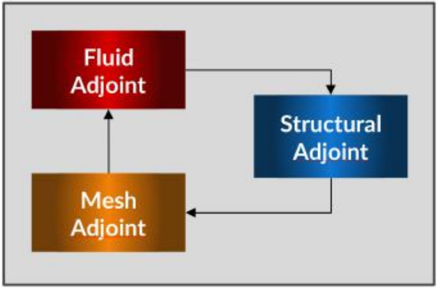

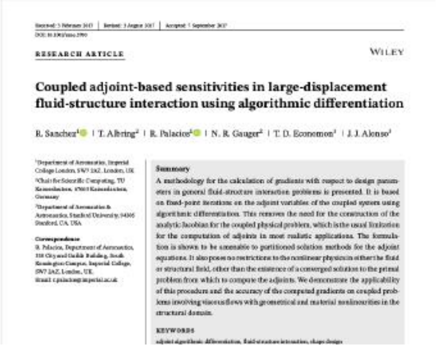

RESEARCH ARTICLE

WILEY

Coupled adjoint-based sensitivities in large-displacement fluid-structure interaction using algorithmic differentiation

R. Sanchez[1] | T. Albring[2] | R. Palacios[1] | N. R. Gauger[2] | T. D. Economon[3] | J. J. Alonso[3]

[1]Department of Aeronautics, Imperial College London, SW7 2AZ, London, UK
[2]Chair for Scientific Computing, TU Kaiserslautern, 67663 Kaiserslautern, Germany
[3]Department of Aeronautics & Astronautics, Stanford University, 94305 Stanford, CA, USA

Correspondence
R. Palacios, Department of Aeronautics, 338 City and Guilds Building, South Kensington Campus, Imperial College, SW7 2AZ, London, UK.
Email: r.palacios@imperial.ac.uk

Summary
A methodology for the calculation of gradients with respect to design parameters in general fluid-structure interaction problems is presented. It is based on fixed-point iterations on the adjoint variables of the coupled system using algorithmic differentiation. This removes the need for the construction of the analytic Jacobian for the coupled physical problem, which is the usual limitation for the computation of adjoints in most realistic applications. The formulation is shown to be amenable to partitioned solution methods for the adjoint equations. It also poses no restrictions to the nonlinear physics in either the fluid or structural field, other than the existence of a converged solution to the primal problem from which to compute the adjoints. We demonstrate the applicability of this procedure and the accuracy of the computed gradients on coupled problems involving viscous flows with geometrical and material nonlinearities in the structural domain.

KEYWORDS
adjoint, algorithmic differentiation, fluid-structure interaction, shape design

For details of coupled-adjoint formulation:

R. Sanchez, T. Albring, R. Palacios, N.R. Gauger, T.D. Economon, J.J. Alonso *"Coupled Adjoint-Based Sensitivities in Large-Displacement Fluid-Structure Interaction Using Algorithmic Differentiation"*, International Journal of Numerical Methods in Engineering, Vol. 113, No. 7, 2017

Coupled FSI Adjoint Solver based on Algorithmic Differentiation

Electro-mechanically Actuated Membrane Wings

R. Sanchez, R. Palacios, T. D. Economon, J. J. Alonso, T. Albring and N. R. Gauger

Optimal Actuation of Dielectric Membrane Wings using High-Fidelity Fluid-Structure Modelling
AIAA paper 2017-0857, presented at Scitech 2017

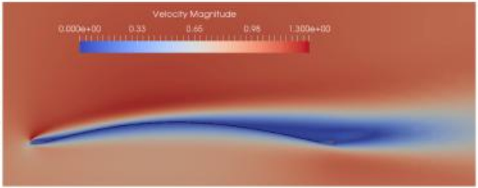

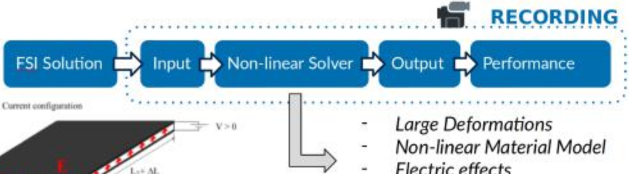

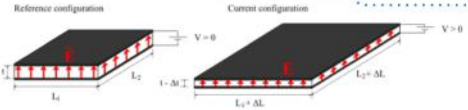

- *Large Deformations*
- *Non-linear Material Model*
- *Electric effects*
- *Viscous flow*

Shape Optimization of FSI

Optimization problem

Area ($A \geqslant A_0$), lift ($c_l = 0.5$), and deformation ($\delta_{TE} \leqslant \delta_{max}$) constrained, drag minimization. Constraints at low Mach number (0.25), objective at high (0.75).

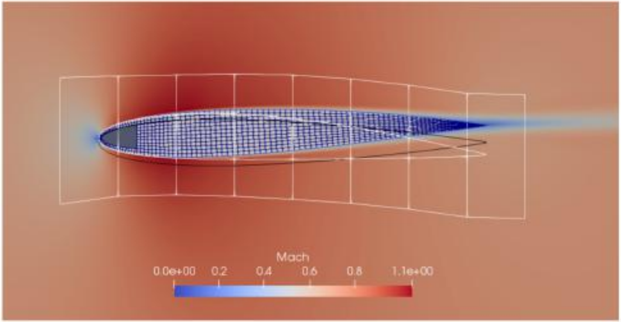

*Preliminary Results from Pedro Gomez & Rafael Palacios (Imperial College London)

Shape Optimization of FSI

δ_{max}	$\mathbf{c_d^{0.75M}}$	$c_l^{0.75M}$	$c_d^{0.25M}$
10.0 mm	**0.008582**	0.07554	0.01117
6.0 mm	**0.008766**	0.1477	0.01128

T.E. displacement constrained to 10mm

T.E. displacement constrained to 6mm

*Preliminary Results from Pedro Gomez & Rafael Palacios (Imperial College London)

Topology Optimization of FSI

Fixed external shape of the 6 mm case, elasticity modulus doubled, weighted objective (80% drag, 20% mass).

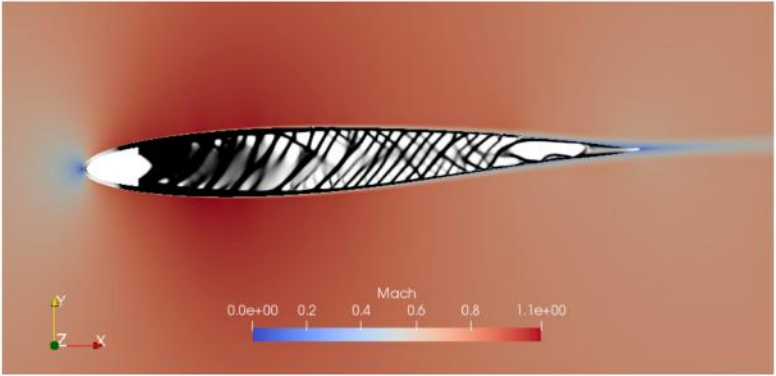

*Preliminary Results from Pedro Gomez & Rafael Palacios (Imperial College London)

Conjugate Heat Transfer

Contributors:

- Ole Burghardt, Tim Albring, Nicolas Gauger (TU Kaiserslautern)

Point of Contact:

Ole Burghardt: ole.burghardt@scicomp.uni-kl.de

Heated Cylinder in Fluid Flow – A Multi-Zone Problem

Let

- $\mathcal{G}^{(1)}$ be a **RANS solver** and
- $\mathcal{G}^{(2)}$ a **heat solver**,

both coupled by transferring temperature and heat flux data at their interface.

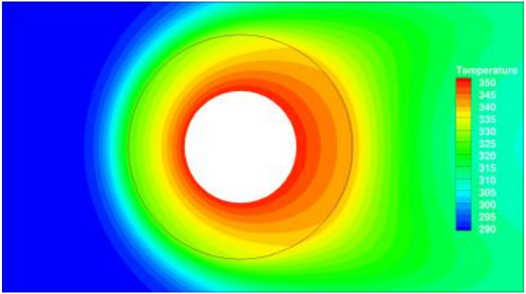

- $D = 0.5\text{m}, \ D_c = 0.25\text{m}$
- $V_\infty = 3.4\frac{m}{s}$, $\text{Re} = 40$
- $T_\infty = 288.15$, $T_c = 350K$
- same material properties, except $\lambda_s = 5\lambda_f$

3D Test Case

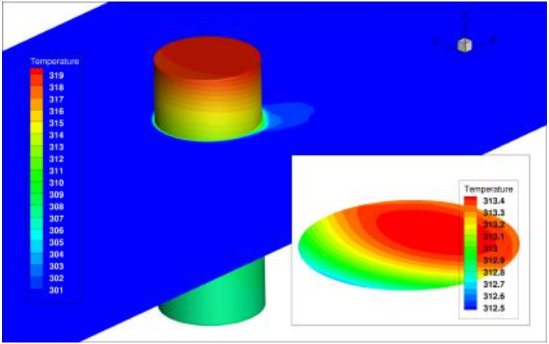

- Heated aluminum cylinder (height/diameter: 5mm/2mm)
- Coolant: water with inflow conditions set at 0.25 m/s, 300K (incompressible solver)
- 4W heat load applied at tip of the pin
- Equilibrium at mean tip temperature of 319K (good agreement with FLUENT)

Coupling under Unsteady and Turbulent Flow Conditions

By its dual-time stepping approach,

- a steady simulation can easily be turned into an unsteady one

and by its modular design,

- other kinds of solvers can be chosen easily.

In the example, change the Reynolds number to 1000 and (optionally) set

```
KIND_TURB_MODEL= SA
HYBRID_RANSLES= SA_EDDES
```

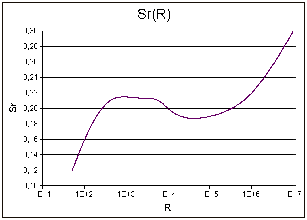

Transient Conjugate Heat Transfer

Based on a Strouhal number of 0.21, we expect a frequency of 1.4Hz, so let us repeat the CHT test case with physical time steps of 0.03s (in total 45s).

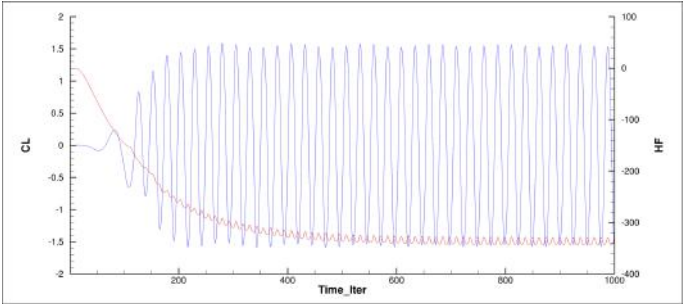

(Initial temperature of the cylinder set to 288.15K.)

Now that we are able to compute accurate primal solutions, can we use our solver to also compute accurate gradients?

Yes, by discrete adjoint solutions based on the same fixed point iterator $\mathcal{G}$.

Discrete Adjoint for Multi-Zone Problems

From an abstract point of view,

$$\lambda \overset{!}{=} \nabla_u \tilde{J}(X,U) + D_u \tilde{\mathcal{G}}^T(X,U) \cdot \lambda$$

also is covering the case where $\mathcal{G}$ is the combination of several $\mathcal{G}^{(k)}$, i.e. we need an implementation of

$$\lambda_{(k)}^{(n+1)} = \frac{\partial \tilde{J}^T}{\partial u_{(k)}}(X,U) + \frac{\partial \mathcal{G}^T}{\partial u_{(k)}}(X,U) \cdot \lambda^{(n)}$$

Though attention has to paid to **evaluate all derivatives correctly** (the full vectors λ and $\partial\mathcal{G}/\partial u_{(k)}$, involving cross dependencies, appear on the right side).

Adjoint Sensitivities for Conjugate Heat Transfer

In our 2D-CHT example,

- $\frac{\partial}{\partial u^{(1)}}\mathcal{G}^{(2)}$ constitutes the heat solver's dependence on the heat fluxes and
- $\frac{\partial}{\partial u^{(2)}}\mathcal{G}^{(1)}$ constitutes the flow solver's dependence on the temperature distribution at the interface,

giving the coupled adjoint solution $\left(\lambda_{(1)}, \lambda_{(2)}\right)$. E.g., for J being the heatflux, the deduced sensitivities have contributions from both zones:

Conjugate Heat Transfer in SU2

Reference

O. Burghardt, N.R. Gauger, "*Accurate gradient computations for shape optimization via discrete adjoints in CFD-related multiphysics problems*", Notes on Numerical Fluid Mechanics and Multidisciplinary Design, No. 142, 2018.

Future Work

- Couple CHT and turbomachinery functionalities for cooled turbine blade optimizations

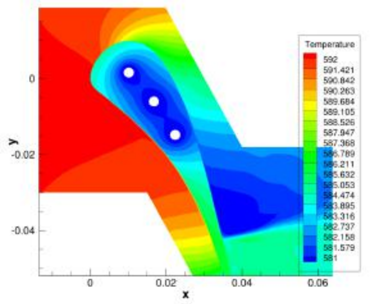

NonEquilibrium MOdels (SU2-NEMO)

Contributors:

- Catarina Garbacz, Marco Fossati (University of Strathcylde)
- Walter T. Maier, Juan J. Alonso (Stanford University)
- James B. Scoggins (École Polytechnique)
- Thomas D. Economon (Bosch)
- Thierry Magin (Von Karman Institute)

Point of Contact:

Marco Fossati: marco.fossati@strath.ac.uk

Basis of SU2-NEMO

Initial efforts by Sean Copeland (PhD, 2015, Stanford University): "A Continuous Adjoint Formulation for Hypersonic Flows in Thermochemical Nonequilibrium"

- continuum, steady, viscous, multi-component, gas mixture in thermochemical nonequilibrium
- Transport properties
  - Diffusion — Fick's Law w/ closure terms
  - Viscosity — Newtonian fluid w/ Stokes' Hypothesis
  - Thermal Cond. — Fourier's Law
- Transport coefficients: Blottner/Eucken + Wilke's semi- empirical mixing rule
- Landau-Teller vibrational relaxation with Park's limiting cross section
- Finite-rate chemistry (Arrhenius-type)
- Derivation of continuous adjoint system

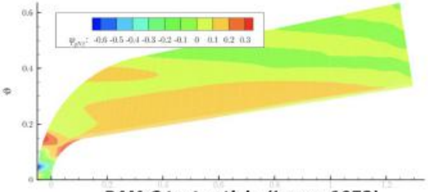

RAM-C test article (Jones, 1972)

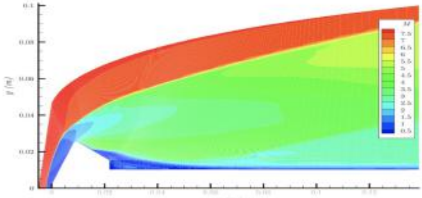

Mars entry vehicle, M = 7.7

Coupling with Mutation++

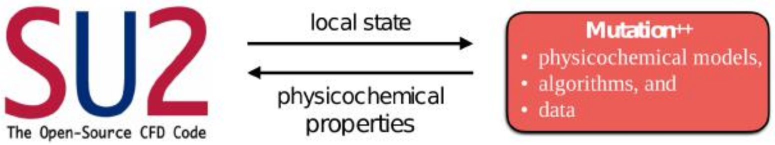

Mutation++: An open-source library developed at VKI, designed to couple with conventional CFD codes to provide thermodynamic, transport, chemistry, and energy transfer properties associated with subsonic to hypersonic flows.

- Thermodynamic properties
- Multicomponent transport properties
- Finite rate chemistry in thermal nonequilibrium
- A robust multiphase equilibrium solver

Hypersonic Double Wedge Configuration

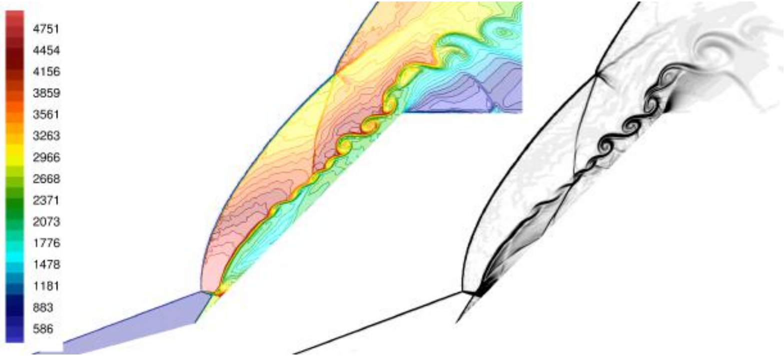

a) Temperature [K]   b) Numerical Schlieren

- Mach 9
- Nonequilibrium shock interference patterns
- 5-Species, (79% N2, 21% O2) freestream

Towards Hypersonic Vehicle Design

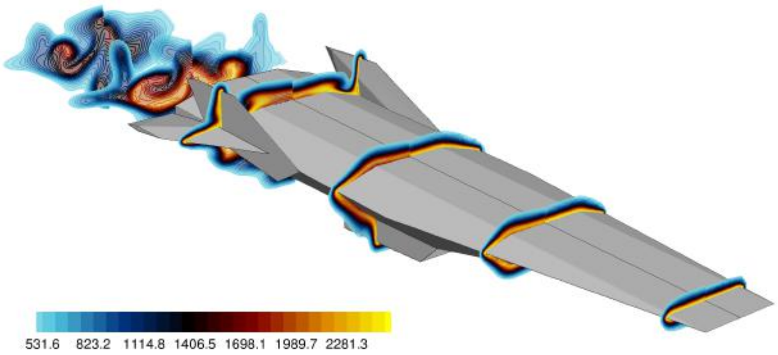

- Grid independence study on X43-like hypersonic vehicle and access-to-space systems

On-Going Efforts

- Implementation of subsonic, characteristic-based outlet boundary
- Validation and verification of Navier-Stokes solver/boundary conditions (Space shuttle wing or Mars entry vehicle)
- Discrete adjoint sensitivity (Validate using RAM-C II case)
- Verify TNE2 source terms at low speed/temperature regimes
- Transitional flow prediction using RANS-style modeling

Helicopter Blade Kinematics

Contributors:

- Myles Morelli, Alberto Guardone (Politecnico di Milano)

Point of Contact:

Myles Morelli: mylescarlo.morelli@polimi.it

Helicopter Blade Kinematics in Forward Flight

- In forward flight, experience a blade normal velocity which depends on the azimuthal position:

$$M_n(\psi) = M_{tip}\frac{r}{R} + M_\infty sin\psi = M_{tip}\left(\frac{r}{R} + \mu sin\psi\right)$$

- The differences in the blade normal velocities combined with the requirement that the rotor does not produce pitching or rolling moments is the main challenge.
- Flapping hinge introduced eliminating the rolling moment which arises in forward flight. Flapping causes large Coriolis moments in the plane of rotation and the lag hinge is provided to relieve these moments. Lastly the pitching hinge allows the blade to be pitched.

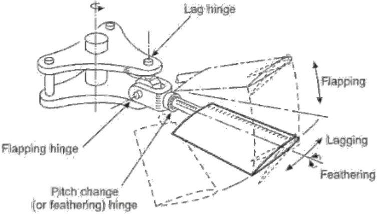

Helicopter Blade Kinematics in Forward Flight

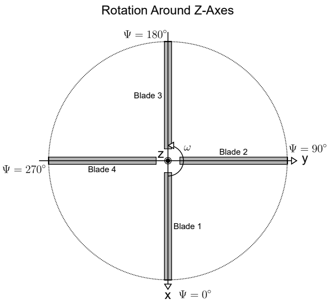

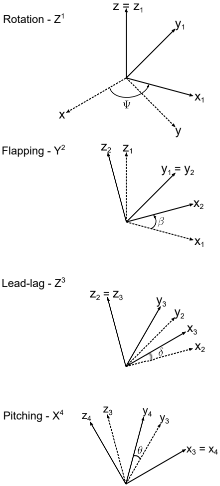

Rotation Matrix Z^1-Y^2-Z^3-X^4

- Modeled within SU2 using a helicopter fixed-frame of reference
- Blades are rotating around the z-axis
- The order of the flapping, lead-lag and pitching motion is important.

Helicopter Blade Kinematics in Forward Flight

```
CIteration::~CIteration(void) { }

void CIteration::SetGrid_Movement(CGeometry ****geometry_container,
         CSurfaceMovement **surface_movement,
         CVolumetricMovement ***grid_movement,
         CFreeFormDefBox ***FFDBox,
         CSolver *****solver_container,
         CConfig **config_container,
         unsigned short val_iZone,
         unsigned short val_iInst,
         unsigned long IntIter,
         unsigned long ExtIter)   {

  case ROTORCRAFT:
    if (rank == MASTER_NODE){
      cout << "Updating grid into hub reference system." << endl;
      grid_movement[val_iZone][val_iInst]->Blade_Rotation(geometry_container[val_iZone][val_iInst][MESH_0],
                                              config_container[val_iZone], val_iZone, ExtIter);

      cout << "Updating blade surfaces into blade reference systems. " << endl;
      surface_movement[val_iZone]->Blade_Kinematics(geometry_container[val_iZone][val_iInst][MESH_0],
                                          config_container[val_iZone], ExtIter, val_iZone);

      cout << "Deforming the volume grid. " << endl;
      grid_movement[val_iZone][val_iInst]->SetVolume_Deformation(geometry_container[val_iZone][val_iInst][MESH_0],
                                                  config_container[val_iZone], true);

      grid_movement[val_iZone][val_iInst]->UpdateMultiGrid(geometry_container[val_iZone][val_iInst], config_container[val_iZone]);
    }

    break;
}
```

- Created a new grid movement type called ROTORCRAFT
- At each iteration, apply the blade rotation as a volumetric grid movement
- Then apply the blade kinematics as a surface movement.

Helicopter Blade Kinematics in Forward Flight

```
% ----------------------- DYNAMIC MESH DEFINITION -----------------------------%
%
% Dynamic mesh simulation (NO, YES)
GRID_MOVEMENT= YES
%
% Type of mesh motion (NONE, FLUTTER, RIGID_MOTION, FLUID_STRUCTURE,
% ROTORCRAFT)
GRID_MOVEMENT_KIND= ROTORCRAFT
%
% Definition of coordinate system. Defined by which axis the rotation occurs on
% (X_AXIS, Y_AXIS, Z_AXIS)
COORD_SYS= Z_AXIS
%
% Angular velocity vector (rad/s) about the hub origin
BLADE_ROTATION_RATE_X= 0.0
BLADE_ROTATION_RATE_Y= 0.0
BLADE_ROTATION_RATE_Z= 180.0
%
% Coordinates of the hub origin
HUB_ORIGIN_X= 0.0
HUB_ORIGIN_Y= 0.0
HUB_ORIGIN_Z= 0.0
%
% Coordinates of the first hinge origin
HINGE_ORIGIN_X= 0.0
HINGE_ORIGIN_Y= 0.0
HINGE_ORIGIN_Z= 0.0
%
% Blade phase offset (degrees) about the azimuth angle
% e.g. A four-bladed rotor (0 90 180 270)
BLADE_PHASE_X= 0.0 0.0
BLADE_PHASE_Y= 0.0 0.0
BLADE_PHASE_Z= 90.0 270.0
% Coefficients of the equations of the blades pitching motion and higher harmonics
% Format -> theta(psi) = theta_0 - theta_1s sin(psi) - theta_1c cos(psi) ...
BLADE_PITCH_MOTION= 4.0 2.0 0.0
%
% Coefficients of the equations of the blades flapping motion and higher harmonics
% Format -> beta(psi) = beta_0 - beta_1s sin(psi) - beta_1c cos(psi) ...
BLADE_FLAP_MOTION= 2.0 2.0 2.0
%
% Coefficients of the equations of the blades lead-lag motion and higher harmonics
% Format -> delta(psi) = delta_0 - delta_1s sin(psi) - delta_1c cos(psi) ...
BLADE_LEADLAG_MOTION= 0.0 -2.0 0.0
%
% Moving wall boundary marker(s) (NONE = no marker, ignored for RIGID_MOTION)
MARKER_MOVING=( blade_1, blade_2 )
```

- New config options required for a ROTORCRAFT simulation

Helicopter Blade Kinematics in Forward Flight

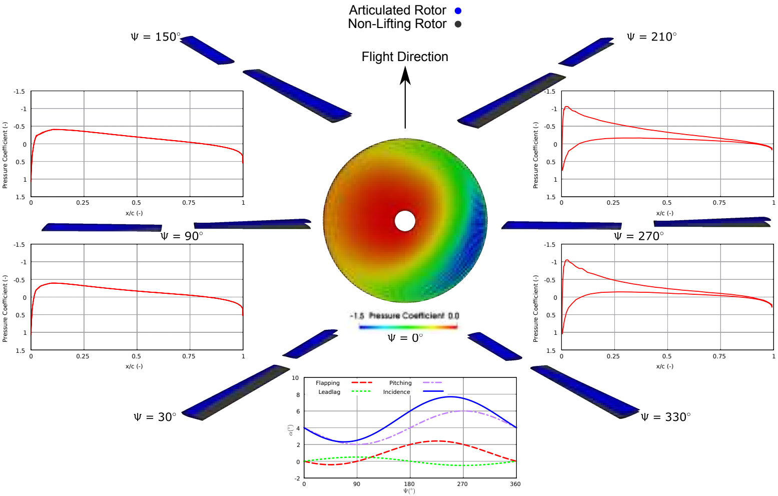

- Caradonna-Tung rotor with untwisted NACA0012 airfoil, rotating CCW
- Mesh available in TestCase folder

Helicopter Blade Kinematics in Forward Flight

Reference

M. Morelli, T. Bellosta, and A. Guardone, "*Lagrangian Particle Tracking in Deforming Sliding Mesh for Rotorcraft Icing Applications*", In: 45th European Rotorcraft Forum, Warsaw Poland, September 2019.

Future Work

- Validate the flow field of the resultant blade kinematics. HART-II experimental test campaign has been selected. This experimental test case will also allow us to assess the acoustics produced from the main rotor in descending flight when strong BVI is present.
- Once at a stage where there is complete verification of the method and validation of the results there will be a pull request to merge the feature_ROTORCRAFT branch into the main release branch.
- Modeling the elastic nature of the rotor blades is also being considered through the coupling of the open-source multibody dynamics software, MBDyn with SU2 using the open-source coupling library, preCICE.
- Rotor blade shape optimization to improve aerodynamic and aeroacoustic performance (joint work with Beckett Y. Zhou, TU Kaiserslautern)